

A NOVEL SYMMETRY IN NANOCARBONS: PRE-CONSTANT DISCRETE PRINCIPAL CURVATURE STRUCTURE

YUTARO KABATA, SHIGEKI MATSUTANI, YUSUKE NODA, YUTA OGATA, JUN ONOE

ABSTRACT. Since the first-principles calculations in quantum chemistry precisely provide possible configurations of carbon atoms in nanocarbons, we have analyzed the geometrical structure of the possible carbon configurations and found that there exists a novel symmetry in the nanocarbons, i.e., the pre-constant discrete principal curvature (pCDPC) structure. In terms of the discrete principal curvature based on the discrete geometry for trivalent oriented graphs developed by Kotani, Naito, and Omori [Comput. Aided Geom. Design, **58**, (2017), 24-54], we numerically investigated discrete principal curvature distribution of the nanocarbons, C_{60} , carbon nanotubes, C_{120} (C_{60} dimer), and C_{60} -polymers (peanut-shaped fullerene polymers). While the C_{60} and nanotubes have the constant discrete principal curvature (CDPC) as we expected, it is interesting to note that the C_{60} -polymers and C_{60} dimer also have the almost constant discrete principal curvature, i.e., pCDPC, which is surprising. A nontrivial pCDPC structure with revolutionary symmetry is available due to discreteness, though it has been overlooked in geometry. In discrete geometry, there appears a center axisoid which is the discrete analogue of the center axis in the continuum differential geometry but has three-dimensional structure rather than a one-dimensional curve due to its discrete nature. We demonstrated that such pCDPC structure exists in nature, namely in the C_{60} -polymers. Furthermore, since we found that there is a positive correlation between the degree of the CDPC structure and stability of the configurations for certain class of the C_{60} -polymers, we also revealed the origin of the pCDPC structure from an aspect of materials science.

1. INTRODUCTION

Interdisciplinary field between mathematics and materials science has recently been attracted. Especially geometrical properties of carbon networks determine their material properties [1]. The relations between carbon networks and discrete differential geometry are currently concerned after Terrones and Mackay proposed a carbon network, which is supposed to be a discrete version of the Schwarzian surface, a triply periodic minimal surface with negative Gaussian curvature; it is known as the classical Mackay crystal [2, 3]. Further K_4 crystal was theoretically proposed based on mathematical consideration, and its properties were studied by the first-principles calculations [4], though it is unstable from the viewpoint of phonon dispersion [5]. Recently Kotani, Naito and Omori developed excellent tools in the discrete differential geometry for trivalent graphs embedded in three-dimensional euclidean space \mathbb{R}^3 , and investigated the carbon networks in terms of the discrete differential geometry [6, 7]. Furthermore, Sunada also described mathematical structures behind them [8]. However, there have been no geometrical analyses of the

Date: June 30, 2023.

actual nanocarbon geometry obtained by the first-principles calculations as far as we know.

In this paper, we have investigated the discrete differential geometrical properties of nanocarbons, mainly C_{60} -polymers extended to the one-dimensional direction due to the linkage among C_{60} s, by using the data of the actual nanocarbon geometry obtained by first-principles calculations. Such an analysis is the first attempt as far as we know.

The C_{60} -polymers are sometimes referred to as the peanut-shaped fullerene polymer (PSFP) due to their shape. The C_{60} -polymer were discovered in 2003 [9, 10], which have been produced by electron beam irradiation of C_{60} thin films [9]. The electron system on the C_{60} -polymer exhibits Tomonaga-Luttinger liquid states, which has a novel behavior due to the submanifold quantum system different from conventional nanocarbons such as nanocarbons, nanotubes, and graphene [11], and thus it is fascinating to understand its geometrical property but it has never been revealed yet. Since the atomic configurations of the C_{60} -polymers were determined by the first principles calculations [12, 13], we investigate the differential geometrical properties of the C_{60} -polymers by analyzing the atomic configuration data in terms of the discrete geometrical tools introduced by Kotani, Naito and Omori [6]. Such a discrete differential geometrical analysis on the atomic configurations given by the first principles calculations is crucial and novel so far.

As shown in Figure 1, the carbon atoms in the C_{60} -polymer look like the boundary surface of a solid of revolution. It may be decomposed to three regions from a continuum geometrical viewpoint, i.e., the elliptic region (positive Gauss curvature), the parabolic region (null-Gauss curvature), and the hyperbolic (negative Gauss curvature). The shape might be similar to the Delaunay surface, or a constant mean curvature (CMC) surface. Though there have been several reports on the relation between carbon networks (or nanocarbons) and the Delaunay surfaces, [14, 15], our numerical analysis showed that the shape of the C_{60} -polymer cannot be regarded as the Delaunay surface as will be mentioned in this paper. However, instead of the CMC property, the geometrical analysis of the first-principles computational results leads to a novel property that shows almost constant discrete principal curvature due to its discrete nature; we refer to it as *pre-constant discrete principal curvature (pCDPC)*.

To the best of our knowledge, the pCDPC surfaces have never been mentioned in any literature so far. It is a novel symmetry of carbon atom networks, which has neither been investigated anyplace.

Hence, we have further investigated the geometrical properties of the typical kinds of the nanocarbons, i.e., C_{60} , C_{60} -dimer, nanotubes the C_{60} -polymers in terms of tools in [6], and found that the novel geometrical structure, the pCDPC, also holds in all of those nanocarbons. This finding is interesting since those nanocarbons have the pCDPC, which has never been described. In other words, the geometrical properties can be regarded as a novel discrete geometrical symmetry hidden in the nanocarbons. It is emphasized that this symmetry was first discovered by an interdisciplinary study between geometry and materials science in this paper. We report this symmetry in this paper.

The contents of this paper is following. Section 2 is a mathematical preliminary to show the discrete geometrical properties following Kotani, Naito, and Omori [6, 16]. We review the shapes of the C_{60} -polymers obtained using the first-principles calculations as

in [13] in Section 3. By the discrete geometrical analysis, the geometrical properties of the C_{60} -polymers, and C_{60} -dimer (C_{120}), and nanotubes are shown in Sections 4 and 5. Thereafter, we discuss these results in Section 6. Finally, we describe the conclusions and perspectives in the present study in Section 7.

2. MATHEMATICAL PRELIMINARY

In this section, we review the discrete differential geometry of trivalent oriented graphs embedded into the three-dimensional euclidean space \mathbb{R}^3 following Kotani, Naito and Omori [6]. We refer to it as KNO construction, and based on it, we introduce the discrete principal curvature as follows [16]:

Let $X = (V_X, E_X)$ be a trivalent oriented graph; for each vertex $x \in V_X$, we have the subset of edges $E_x = \{e_1, e_2, e_3\} \subset E_X$ whose incident point is x , i.e., $x = t(e_i)$. The orientation is determined so that each cycle in X is consistent.

We consider the embedding $\iota : X \rightarrow \mathbb{R}^3$; we denote $\iota(x)$ by \mathbf{x} and $\iota(e)$ by \mathbf{e} for $x \in V_X$ and $e \in E_X$. The tangent plane $T_{\mathbf{x}}$ with the normal vector $\mathbf{n}_x \in \mathbb{R}^3$ at \mathbf{x} is defined by

$$\mathbf{n}_x = \frac{(\mathbf{e}_1 - \mathbf{e}_3) \wedge (\mathbf{e}_2 - \mathbf{e}_3)}{|(\mathbf{e}_1 - \mathbf{e}_3) \wedge (\mathbf{e}_2 - \mathbf{e}_3)|} = \frac{\mathbf{e}_1 \wedge \mathbf{e}_2 + \mathbf{e}_2 \wedge \mathbf{e}_3 + \mathbf{e}_3 \wedge \mathbf{e}_1}{|\mathbf{e}_1 \wedge \mathbf{e}_2 + \mathbf{e}_2 \wedge \mathbf{e}_3 + \mathbf{e}_3 \wedge \mathbf{e}_1|}$$

for $\mathbf{e}_i = \iota(e_i)$ of $E_x = \{e_1, e_2, e_3\}$. For $x \in V_X$ and $E_x = \{e_1, e_2, e_3\} \subset E_X$, let each adjacent vertex be denoted by x_i , i.e., $e_i = (x, x_i)$, ($i = 1, 2, 3$) so that the ordered vertices x_1, x_2, x_3 form an oriented triangle Δ_x given by $\mathbf{x}_i = \iota(x_i)$, ($i = 1, 2, 3$), i.e., $\Delta_x = (\mathbf{x}_1, \mathbf{x}_2, \mathbf{x}_3) \subset \mathbb{R}^3$. For each \mathbf{x}_i , the normal vector $\mathbf{n}_i = \mathbf{n}_{x_i}$, ($i = 1, 2, 3$) is assigned. We set $\mathbf{v}_1 = \mathbf{e}_1 - \mathbf{e}_3 = \mathbf{x}_1 - \mathbf{x}_3$ and $\mathbf{v}_2 = \mathbf{e}_2 - \mathbf{e}_3 = \mathbf{x}_2 - \mathbf{x}_3$. Let the euclidean inner product be $\langle \cdot, \cdot \rangle : \mathbb{R}^3 \times \mathbb{R}^3 \rightarrow \mathbb{R}$. We introduce the discrete first fundamental form I_x defined by

$$I_x = (g_{ij}) = \begin{pmatrix} \langle \mathbf{v}_1, \mathbf{v}_1 \rangle & \langle \mathbf{v}_1, \mathbf{v}_2 \rangle \\ \langle \mathbf{v}_2, \mathbf{v}_1 \rangle & \langle \mathbf{v}_2, \mathbf{v}_2 \rangle \end{pmatrix}.$$

We also define the directional derivative $\nabla_i \mathbf{n}_x$ of the normal vector \mathbf{n} for the vector \mathbf{v}_i by

$$\nabla_i \mathbf{n}_x = \text{Proj}_x[\mathbf{n}_i - \mathbf{n}_3] = (\mathbf{n}_i - \mathbf{n}_3) - \langle \mathbf{n}_i - \mathbf{n}_3, \mathbf{n}_x \rangle \mathbf{n}_x$$

for $i = 1, 2$; we note that Proj_x exhibits the orthogonal projection onto the tangent plane $T_{\mathbf{x}}$. The discrete second fundamental form II_x is defined by

$$\begin{aligned} II_x &= - \begin{pmatrix} \langle \mathbf{v}_1, \nabla_1 \mathbf{n}_x \rangle & \langle \mathbf{v}_1, \nabla_2 \mathbf{n}_x \rangle \\ \langle \mathbf{v}_2, \nabla_1 \mathbf{n}_x \rangle & \langle \mathbf{v}_2, \nabla_2 \mathbf{n}_x \rangle \end{pmatrix} \\ &= - \begin{pmatrix} \langle \mathbf{v}_1, \mathbf{n}_1 - \mathbf{n}_3 \rangle & \langle \mathbf{v}_1, \mathbf{n}_2 - \mathbf{n}_3 \rangle \\ \langle \mathbf{v}_2, \mathbf{n}_1 - \mathbf{n}_3 \rangle & \langle \mathbf{v}_2, \mathbf{n}_2 - \mathbf{n}_3 \rangle \end{pmatrix}. \end{aligned}$$

The discrete Weingarten map is introduced by $\Gamma_x = I_x^{-1} II_x$. Using Γ_x , the discrete mean curvature H_x and the discrete Gaussian curvature G_x are defined by

$$H_x = \text{tr}(\Gamma_x), \quad G_x = \det(\Gamma_x).$$

Based on the KNO construction [6], the discrete principal curvatures k_1 and k_2 are defined by,

$$(t - k_1)(t - k_2) = t^2 - H_x t + G_x,$$

such that $|k_1| \geq |k_2|$ [16]. They are natural discrete analogue of the principal curvature in the differential geometry, whose inverse should be regarded as the discrete analogue of the curvature radius, i.e., $\rho_a = 1/k_a$ ($a = 1, 2$).

We define the center of the curvature radius $\mathbf{c}_{x,a}$ by

$$\mathbf{c}_{x,a} = \mathbf{x} - \rho_a \mathbf{n}_x. \quad (2.1)$$

Even though the solid of revolution has the center axis, for the discrete analogue $\iota(X)$ of the solid of revolution, the set of $\{\mathbf{c}_{x,1} \mid x \in V_X\}$ does not exist on a straight line, in general. We, thus, refer to the set as the *center-axisoid* [16]. The distribution of the center-axisoid in three dimensional space shows the nature of the discrete geometry.

3. SHAPES OF THE C_{60} -POLYMER OBTAINED USING THE FIRST-PRINCIPLES CALCULATION

In the present work, we have mainly investigated the C_{60} -polymer, which is extended to the one-dimensional direction due to the linkage among C_{60} s, illustrated in Figure 1. The C_{60} -polymers are produced by irradiating C_{60} thin films with electron beams [9]. The shape of the C_{60} -polymers has been confirmed by analysis of infrared spectra in combination with first-principles calculations [17], and of the electron diffraction patterns by the high-resolution transmission electron microscopy and the high-resolution cryo-transmission electron microscopy [18, 19], but the atomic configurations of its geometrical shape are not still determined precisely. Thus we investigate the shapes determined by the first-principles calculation. We analyzed them from a geometrical viewpoint using the tools prepared in the previous section.

However there are several local minimums of the shapes argued in [20, 21, 13]. We have mainly analyzed the shape of FP5N, which has the lowest total energy in the computation but also gave some results for two shapes as references; (later we will consider further 13 shapes in Section 6.)

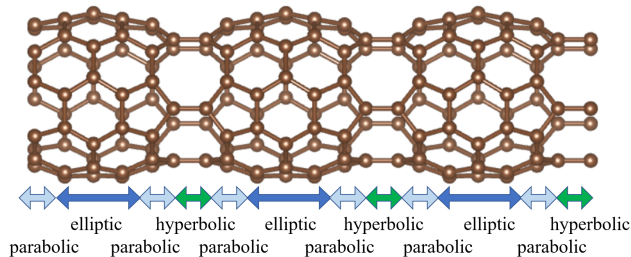


FIGURE 1. The C_{60} -polymers by the first-principles calculation: FP5N [13]

We mention the first-principles calculations in the present work following [13].

The authors in [13] used a generalized Stone-Wales (GSW) transformation to search the smaller energy of the configurations of carbon atoms for the C_{60} -polymers, to which are referred as the PSFP models. They compared their results with those of T3 model of the C_{60} -polymer proposed by Wang and Huang [20]. We also regard it as one of the PSFP models.

Following them, we performed the first-principles calculations in the present work. In the present calculations, we employed Vienna ab-initio simulation package (VASP) [22] based on density functional theory (DFT) [23] to optimize the coordinates of carbon atoms and the volume of a periodic unit cell, and to investigate the energetic properties of the PSFP models. In our DFT calculations, a generalized gradient approximation (GGA) exchange-correlation functional proposed by Perdew, Burke, and Ernzerhof (PBE) [24] and a projector augmented wave (PAW) pseudopotential were used [25]. The three-dimensional periodic unit cell of the rectangular cuboid shape with $L \times 20.000 \times 20.000 \text{ \AA}^3$ was used, where L is a lattice parameter of the primitive C_{60} -polymer region and the L value for each PSFP model is listed in Table 1. A cutoff energy for the plane-wave basis set was set to 500 eV, and a $10 \times 1 \times 1$ Γ -centered k -point grid was used for the geometrical optimization of the PSFP models. The atomic coordinates and the lattice parameters L were optimized with the total energy convergence criterion being 10^{-8} eV between two ionic optimization steps.

The calculated results for three of them are summarized in Table 1, and their shapes are displayed in Figure 2.

TABLE 1. Computational results of the C_{60} -polymers [13]: G , L , $E_{\text{tot,uc}}$, $E_{\text{tot,a}}$, and E_g stand for a symbol of point group symmetry, lattice parameter of the C_{60} -polymer region, total energy per unit cell, total energy per atom, and electronic band gap between valence band maximum and conduction band minimum. The total energy values indicate the energy difference from the total energy of the T3 model.

PSFP	G	L (\AA)	$E_{\text{tot,uc}}$ (eV/cell)	$E_{\text{tot,a}}$ (eV/atom)	E_g (eV)
FP5N	D_{5h}	8.128	-2.177	-0.0363	
FP4L	C_{2h}	8.250	-1.233	-0.0206	0.026
T3	D_{5d}	8.694	0.000	0.0000	1.169

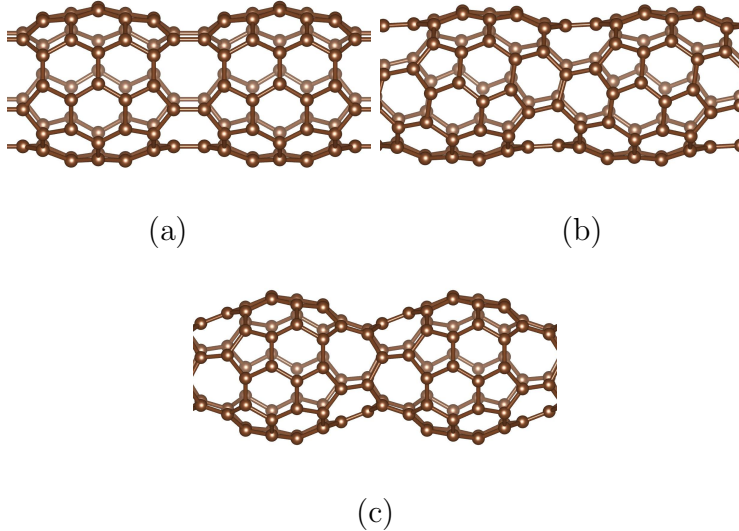


FIGURE 2. The shape of the C_{60} polymers given by the first-principles calculations I:FP5N (a), FP4L (b), and T3 (p).

4. GEOMETRICAL PROPERTIES OF THE C_{60} -POLYMERS

As illustrated in Figure 1, we may observe that the shape of the C_{60} -polymers has the three regions from a continuum geometrical viewpoint; the elliptic region (positive Gauss curvature), the parabolic region (null-Gauss curvature), and the hyperbolic region (negative Gauss curvature). The discrete Gauss curvature G_x is also given by the product of the principal curvatures k_1 and k_2 , i.e., $G_x = k_1 k_2$. We geometrically analyzed the configuration data obtained by the first-principles calculations by using the geometrical tools described in Section 2. We obtained the distributions of the discrete principal curvature of the configuration of the C_{60} -polymers as trivalent regular graphs. Figure 3 displays (a) the numbering of the carbons in the C_{60} -polymer, (b) the distribution of the discrete principal curvature at each carbon, and the frequency of the discrete principal curvatures k_1 and k_2 . As we predicted above, the distribution of the discrete principal curvature shows that the region of the distribution is decomposed into the three regions, $k_1 k_2 > 0$ (elliptic), $k_1 k_2 \sim 0$ (parabolic), and $k_1 k_2 < 0$ (hyperbolic). However it is remarked that the first principal curvature k_1 is almost constant, which is supported by the frequency of the discrete principal curvatures k_1 and k_2 in Figure 3 (c).

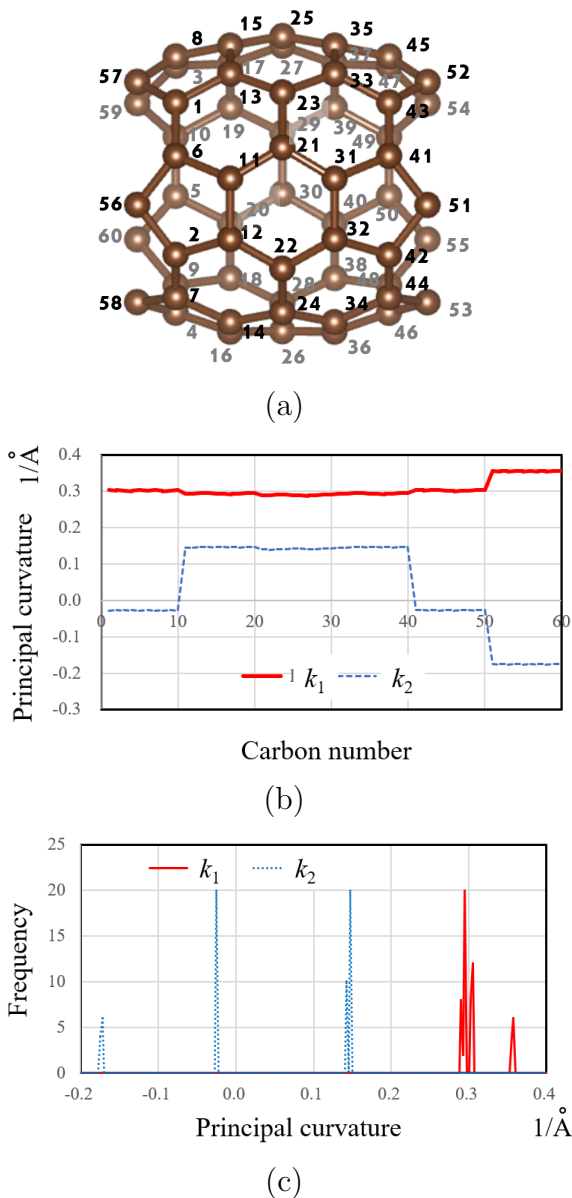


FIGURE 3. The discrete principal curvature distribution of the C_{60} -polymer: (a) shows the numbering of the carbon atoms in the C_{60} -polymer (FP5N), (b) the value of the discrete principal curvatures k_a ($a = 1, 2$) at each carbon atom, and (c) the frequency.

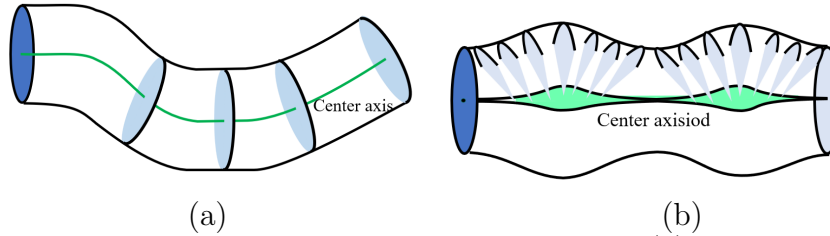


FIGURE 4. Non-trivial CPC and CDPC surfaces: (a) is a CPC surface and (b) is a CDPC surface.

In differential geometry (as continuum theory), it is so strong that the restriction of the principal curvature of surfaces to be constant [16]. The examples of the constant principal curvature surfaces (CPC surfaces) in differential geometry are spheres and cylinders, and non-trivial cases are illustrated in Figure 4 (a). This means that the surface of revolution with CPC structures must be cylinders or spheres only in the continuum geometry.

However, we encounter a different aspect in the discrete geometry. Due to the discrete nature, we may find further non-trivial constant discrete principal curvature (CDPC) surfaces displayed in Figure 4 (b), since the discrete principal curvature is determined locally and the center-axisoid has a nontrivial structure [16]. There appears inconsistency of the center axis of the surfaces of revolution in the discrete versions, which was already remarked by Kotani, Naito and Omori [6] for a nanotube. The structure of the C_{60} -polymer is surely determined by such a discrete nature. We compute the center axisoid of the C_{60} -polymer using the formula (2.1). Figure 5 displays its distributions of the C_{60} -polymer; we found its three dimensional structure rather than one-dimensional line. Even though its shape is not CDPC precisely, the first principal curvature in the C_{60} -polymer of FP5N is almost constant. The existence of the center axisoid provides such co-existence of non-trivial shape of discrete analogue the surfaces of revolution and the almost CPC structure. Thus we refer to the discrete surface as the *pre-constant discrete principal curvature surface (pCDPC surface)* as mentioned in Introduction.

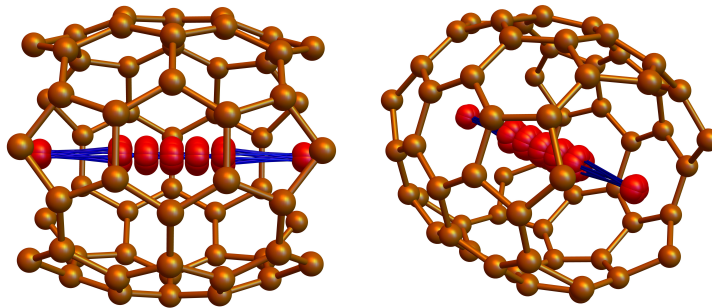


FIGURE 5. Center axisoid of the C_{60} -polymer (FP5N): The carbon atom configuration of FP5N and its center axisoid $\{\mathbf{c}_{x,1}\}$ given by (2.1) are illustrated. Red points show $\{\mathbf{c}_{x,1}\}$.

5. GEOMETRICAL PROPERTIES OF THE NANOCARBONS

Since C_{60} and carbon nanotubes (CNT) are expected to have the CDPC, we evaluate the discrete curvatures in the nanocarbons based on as illustrated in Figure 6 (each arrow indicates a normal vector). Their geometrical structures were determined by the first principles calculations. Here, the parameters are the same as those described above [13]. We examined the two types of the carbon nanotubes as shown in Figures 6 (b) and (c). Nanotube 05-05 consists of ten carbon atoms with one of the edges of the carbon hexagon parallel to the perimeter, whereas nanotube 09-00 has nine perimeter carbon atoms with one of the carbon hexagon parallel to the center axis. Figures 6 (d)-(f) show three types (FP5N, FP4L, and T3) of the peanut-shaped C_{60} polymers, respectively. Figure 6 (g) shows a peanut-shaped C_{60} dimer, (C_{120} , P08) reported previously [17].

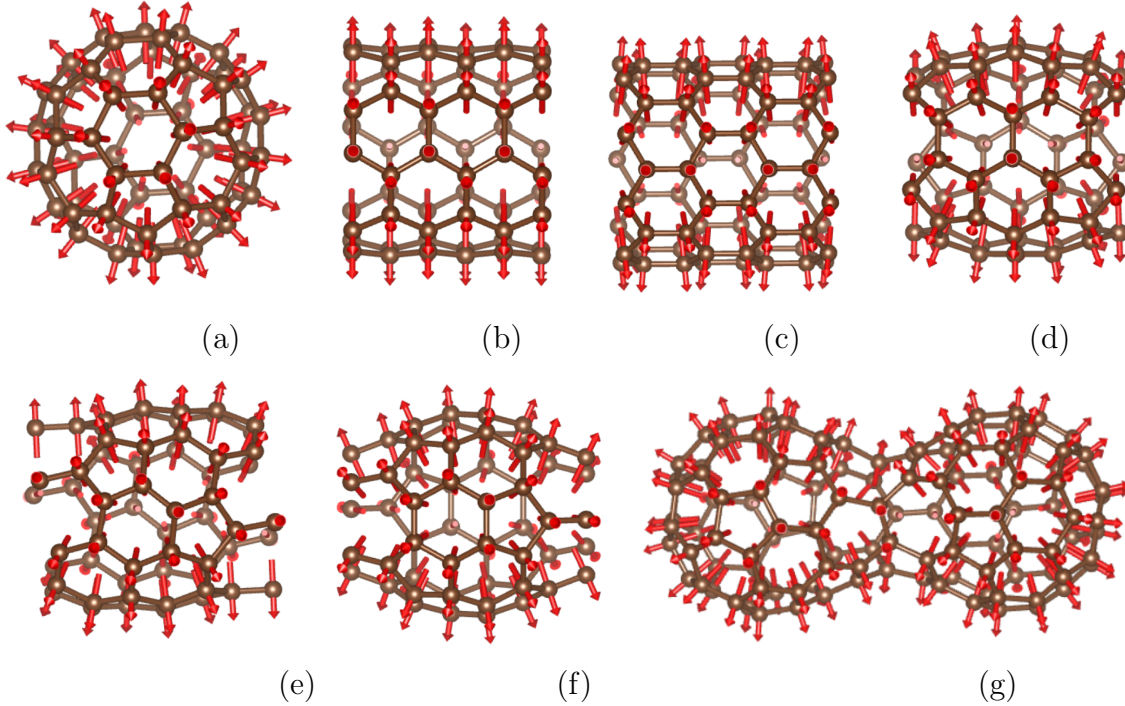


FIGURE 6. The shape of nanocarbons by the first-principles calculations: C_{60} (a), nanotubes 05-05 (b) and 09-00 (c), the C_{60} -polymers, FP5N (d), FP4L (e), T3 (f), and C_{60} dimer (C_{120} , P08) (g). The arrows show the discrete normal vector at each carbon.

The discrete principal curvatures k_1 and k_2 of these nanocarbons are summarized in Table 2; $\overline{k_a}$, $1/\overline{k_a}$, and δk_a denote the average of k_a , the curvature radius, the standard deviation against the carbon atoms, respectively. In order to confirm the calculated results of Table 2, we examined the average and the standard deviation of the angle θ and the bond length a for each bond as shown in Table 3. Since they show the constant length and constant angle, the calculated results are reasonable.

TABLE 2. The discrete principal curvature of the nanocarbons:

Nanocarbons	\bar{k}_1 (\AA^{-1})	δk_1 (\AA^{-1})	$1/\bar{k}_1$ (\AA)	\bar{k}_2 (\AA^{-1})	δk_2 (\AA^{-1})	$1/\bar{k}_2$ (\AA)
C_{60}	0.2875	0.0004	3.4781	0.2740	0.0003	3.6501
CNT 05-05	0.2891	0.0041	3.4586	0.0000	0.0000	—
CNT 09-00	0.2784	0.0070	3.5923	0.0028	0.0008	—
PSFP FP5N	0.3061	0.0224	3.2674	0.0344	0.1207	29.0469
PSFP FP4L	0.3075	0.0344	3.2518	0.0348	0.1263	28.7248
PSFP T3	0.3216	0.0490	3.1092	0.0644	0.1675	15.5097
C_{120} P08	0.3018	0.0404	3.3132	0.1694	0.1592	5.9019

TABLE 3. The angle and bond length of the nanocarbons:

Nanocarbons	$\bar{\theta}$ (rad)	$\delta\theta$ (rad)	\bar{a} (\AA)	δa (\AA)
C_{60}	0.3333	0.0124	1.4349	0.0254
CNT 05-05	0.3333	0.0010	1.4288	0.0006
CNT 09-00	0.3333	0.0027	1.4288	0.0059
PSFP FP5N	0.3333	0.0187	1.4334	0.0279
PSFP FP4L	0.3333	0.0181	1.4342	0.0285
PSFP T3	0.3333	0.0151	1.4360	0.0375
C_{120} P08	0.3333	0.0142	1.4356	0.0286

Accordingly, Table 2 shows the following interesting results:

- (1) Since all of the standard deviation of the first principal curvature of δk_1 is sufficiently smaller than k_1 itself, they are classified to the pCDPC surfaces.
- (2) Since all of the average of k_1 is similar, and its inverse, or the curvature radius is nearly equal to 3.47 \AA of C_{60} , the property does not depend on the computational parameters of the first-principles calculations. Namely, FP5N, FP4L, and T3 have the same property.
- (3) C_{60} and CNTs have the CDPC k_a ($a = 1, 2$) up to computational deviations or discrete nature. [As mentioned in [6], non-trivial center axisoid appears for the CNTs.]

In case of the C_{60} dimer, (C_{120} , P08), the deviation δk_1 of P08 is not small when compared to the others and its distribution as shown in Figure 7, which shows that it may be also referred to the pCDPC surface. Since the CDPC is a special case of pCDPC, it turns out that the nanocarbons we considered have the pCDPC. The geometrical property is fascinating, which has never been mentioned before.

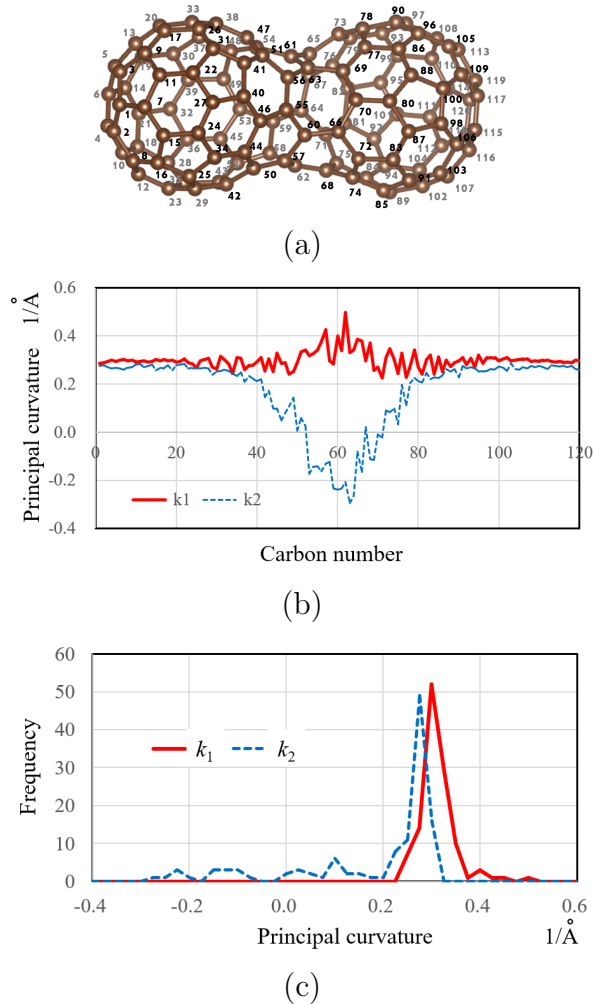


FIGURE 7. The discrete principal curvature distribution of C_{60} dimer, (C_{120} , P08): (a) shows the numbering of the carbon atoms in C_{60} dimer, (C_{120} , P08), (b) the value of the discrete principal curvatures k_a ($a = 1, 2$) at each carbon atom, and (c) the frequency.

6. DISCUSSION

We geometrically analyzed the configuration data of the carbon atoms for the nanocarbons (see Figure 6) and investigated their geometrical properties, especially discrete principal curvature distributions. It is found that all the nanocarbon we investigated have almost constant discrete principal curvature distributions, which are classified to the pCDPC surfaces; Such geometrical property has never been mentioned before. It is due to a nature of the nanocarbons. Since these nanocarbons except two CNTs can be produced from C_{60} via the general Stone-Wales transformation [13], the nature of the nanocarbons is considered to originate from the pCDPC properties.

It is noted that the elliptic ($k_1 k_2 > 0$) region of the C_{60} -polymer and C_{60} dimer (P08) take over the part of C_{60} , and the other parts also preserve the connection as discrete

graphs of C_{60} . On the other hand, under the tight binding picture, the wave functions of each C- $2p$ atomic orbital are affected by the discrete curvature illustrated in Figure 8. The discrete curvature causes the extra overlap integral between adjacent C- $2p$ atomic orbitals, and the total energy correspondingly increases. The discrete curvature expresses the curved carbon networks better than curvature in the continuum picture.

Some restriction of the graph network of C_{60} determines the configuration of the carbon atoms so that the the overlap integral is globally minimized. The directions of the principal curvatures, k_1 and k_2 , are orthogonal to each other, even for the discrete picture [16]. Then, one direction should be chosen because the smaller radius of curvature (or the larger (first) principal curvature, $|k_1| \geq |k_2|$) affects the overlap between adjacent the C- $2p$ atomic orbitals more than the other geometrical parameters, and correspondingly the total energy increases. This indicates that the first discrete principal curvatures should be constant; If a part deviates from the others, the overlap integral has deviation, and the energy density has distribution (not homogeneous). Thus, the first discrete principal curvature tends to be homogeneity. In other words, the nature of the nanocarbon systems originating from C_{60} makes the first discrete principal curvature constant rather than the second one. Therefore, it can be predicted that the total energy would have something to do with the pre-constant first discrete principal curvature property for the C_{60} -polymers and C_{60} -dimer, (C_{120} , P08).

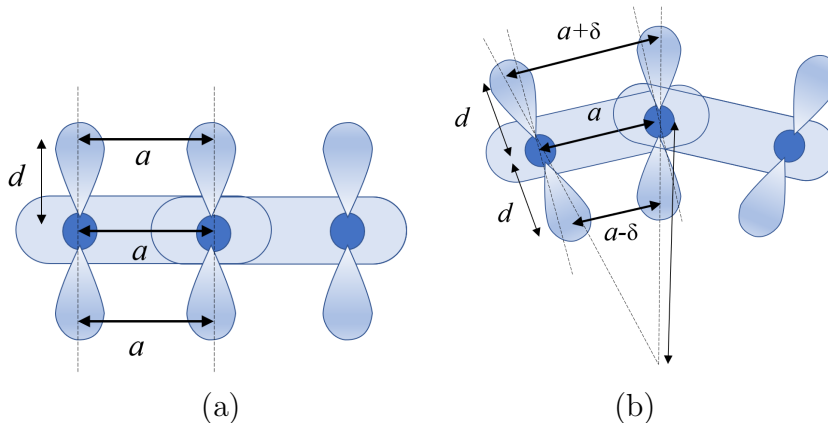


FIGURE 8. The curvature effect on the C- $2p$ atomic orbitals in the tight binding picture: (a) the flat cases, (b) the extra overlap integrals due to the discrete curvature.

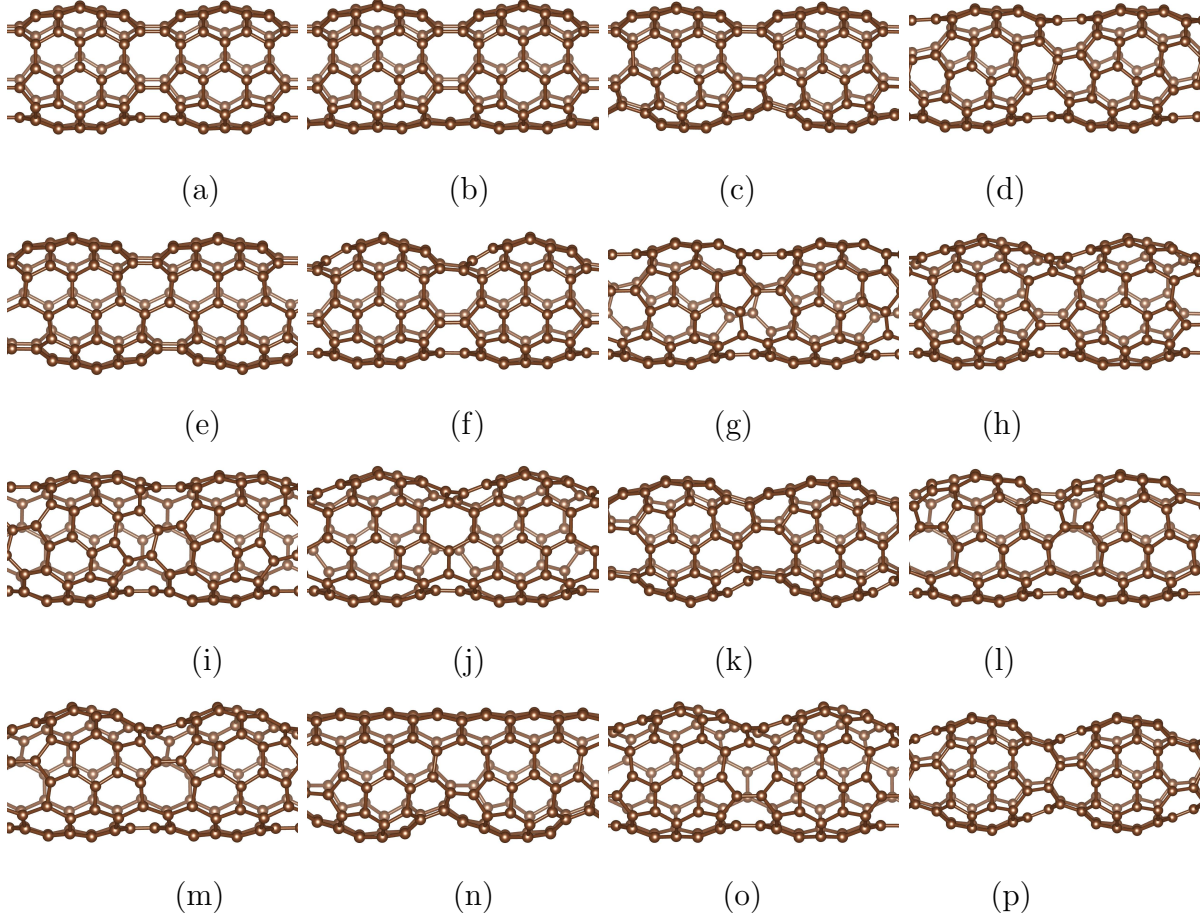


FIGURE 9. The shape of the C_{60} polymers given by the first-principles calculations II: FP5N (a), FP6L (b), FP4K (c), FP4L (d), FP6O (e), FP4J (f), FP5L (g), FP5K (h), FP6F (i), FP6E (j), FP3F (k), FP6J (l), FP6I (m), FP6C (n), FP6K (o), and T3 (p).

Here we analyzed the geometrical configurations of the C_{60} -polymers, or the PSFP models more shown in Table 4, under the same calculation conditions as in Table 1 to clarify the relation between the geometrical properties and the total energy. They have different connections as shown in Figure 9, and thus they have different configurations optimized by the first-principles calculations. The total energy of the nanocarbons lies between those of T3 and FP5N. Since we found no correlations among δk_1 , $\overline{k_1}$, and the total energy per unit cell $E_{\text{tot,uc}}$. Hence we are concerned with the homogeneity of k_1 . It is known that there is a natural graph Laplacian in trivalent graphs. For a function f defined on the vertices on a trivalent graph, the graph Laplacian Δ is defined by

$$(\Delta f)(x) = f(x) - \frac{1}{3}(f(x_1) + f(x_2) + f(x_3)),$$

where x is a centered vertex and x_i 's denote its adjacent varieties. $|\Delta(k_1)|$ shows the degree of the homogeneity for k_1 locally. Then we calculated the average $\overline{|\Delta(k_1)|}$ of $|\Delta(k_1)|$

TABLE 4. Total energy and discrete principal curvature of C₆₀-polymer:

C ₆₀ -P	G	L (Å)	$E_{\text{tot,uc}}$ (eV/cell)	$\overline{k_1}$ (Å ⁻¹)	δk_1 (Å ⁻¹)	$1/\overline{k_1}$ (Å)	$\overline{k_2}$ (Å ⁻¹)	δk_2 (Å ⁻¹)	$1/\overline{k_2}$ (Å)	$ \overline{\Delta k_1} $ (Å)
FP5N	D_{5h}	8.128	-2.177	0.306	0.022	3.267	0.034	0.121	29.047	1.164E-02
FP6L	C_s	7.978	-1.408	0.302	0.021	3.316	0.027	0.114	37.231	1.696E-02
FP4K	C_s	8.244	-1.370	0.306	0.025	3.265	0.036	0.128	27.901	1.583E-02
FP4L	C_{2h}	8.250	-1.233	0.308	0.034	3.252	0.035	0.126	28.725	1.956E-02
FP6O	C_{2h}	7.998	-1.029	0.303	0.026	3.298	0.023	0.105	43.812	1.769E-02
FP4J	C_s	8.210	-0.860	0.308	0.031	3.244	0.040	0.136	25.038	1.860E-02
FP5L	C_1	8.112	-0.803	0.305	0.030	3.280	0.029	0.120	34.045	1.886E-02
FP5K	C_1	8.110	-0.797	0.304	0.026	3.287	0.031	0.121	32.769	1.662E-02
FP6F	C_2	7.917	-0.578	0.300	0.030	3.338	0.025	0.123	40.084	2.042E-02
FP6E	C_1	7.921	-0.452	0.300	0.029	3.328	0.025	0.124	40.567	1.871E-02
FP3F	C_s	8.333	-0.442	0.308	0.028	3.251	0.042	0.140	23.908	1.909E-02
FP6J	C_1	7.936	-0.313	0.299	0.028	3.350	0.024	0.116	41.934	2.176E-02
FP6I	C_1	7.941	-0.184	0.300	0.029	3.335	0.023	0.115	44.278	2.223E-02
FP6C	C_s	7.855	-0.090	0.297	0.030	3.372	0.025	0.136	40.565	1.858E-02
FP6K	C_1	7.939	-0.088	0.300	0.026	3.331	0.023	0.115	44.000	1.971E-02
T3	D_{5d}	8.694	0.000	0.322	0.049	3.109	0.064	0.167	15.510	1.142E-02

against carbon atoms for each C₆₀-polymer, and compared it with the total energy $E_{\text{tot,uc}}$ of the configurations.

Figure 10 shows the correlations between $|\overline{\Delta(k_1)}|$ v.s. the total energy $E_{\text{tot,uc}}$ obtained by the first-principles calculations.

Although T3 data were omitted, we found a strong correlations between them as displayed in Figure 10, which supports the above depiction. Accordingly, it can be concluded that the first principal curvature tends to be homogeneous due to the total energy except the relation between $|\overline{\Delta(k_1)}|$ and $E_{\text{tot,uc}}$ of T3 at this stage. However, it should be emphasized that the pCDPC is revealed to be a novel symmetry of the nanocarbons, which is surely connected with the total energy of the configurations.

This finding was first obtained by the interdisciplinary study between materials science and pure mathematics.

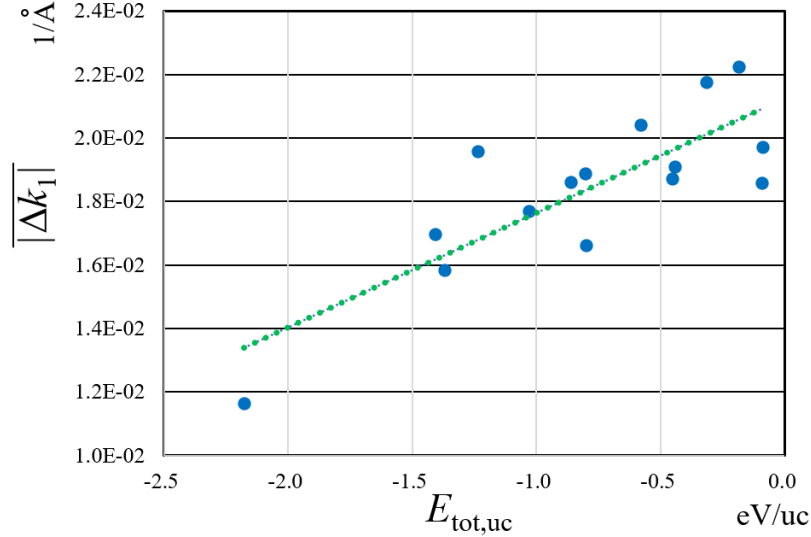


FIGURE 10. Correlation between $E_{\text{tot,uc}}$ and $|\overline{\Delta k_1}|$: except $T3$ in Table 4. ($|\overline{\Delta k_i}| = 0.0036E_{\text{tot,uc}} + 0.0213$, $R^2 = 0.6719$)

7. CONCLUSION

Following the first-principles calculations [13], we recomputed the configurations of the carbon atoms in the nanocarbons, C_{60} , carbon nanotubes, C_{60} dimer, and the C_{60} -polymers. Since the calculations precisely provide possible configurations of carbons in nanocarbons, we analyzed the geometrical structure of the carbon configurations in the nanocarbons. Then we found that there exists a novel symmetry in the nanocarbons, i.e., the pre-constant discrete principal curvature (pCDPC) structure.

Since the discrete geometry for trivalent oriented graphs was introduced by Kotani, Naito, and Omori [6], we defined the discrete principal curvatures k_1 and k_2 based on their results. In terms of the discrete principal curvatures, we numerically investigated the discrete principal curvature distribution of the carbon atom configurations in the nanocarbons by using the data of the first-principles calculations. While the C_{60} and nanotubes have the constant discrete principal curvature we expected, as shown in Table 2, it was shown that the C_{60} -polymers and C_{60} dimer (C_{120}) also have the almost constant discrete principal curvature, i.e., pCDPC, displayed in Figs. 3 and 7. This fact is critical. The nontrivial pCDPC structure is allowed because of its discrete nature. Such a revolutionary geometric symmetry has been overlooked in geometry. In discrete geometry, there appears a center axisoid which is the discrete analogue of the center axis in the continuum differential geometry but has three-dimensional structure rather than a one-dimensional curve due to its discrete nature. We showed that such a symmetry exists in nature, namely in the C_{60} -polymers, which exist in the real world rather than the fictitious world of mathematics. Further, we found that there is a strong correlation

between the degree of the pCDPC structure and stability of the configurations for certain classes of the C_{60} -polymers as in Table 4 and Figure 10. As argued in the Discussion, it could be explained by the overlap of the C- $2p$ atomic orbitals as illustrated in Figure 8. It shows the origin of the pCDPC structure in the nanocarbons.

Moreover, the electric system of the C_{60} -polymers has significant properties arising from the submanifold quantum system [11]. Since the geometrical quantum effects predicted by Jensen and Koppe [26], and da Costa [27] was confirmed experimentally [11], the present study would be extended to the discrete curvature system. Namely, the discrete nature of the electric system of the C_{60} -polymers becomes important to cultivate new novel nanocarbons. For the discrete version of the quantum effects, the path integral method might be proper because the curvature effects appears as the measure of the wave functions and the quantum fields [28, 29].

Acknowledgements: This work was supported by Institute of Mathematics for Industry, Joint Usage/Research Center in Kyushu University. (“IMI workshop II: Geometry and Algebra in Material Science I”, September 7–8, 2020”, (20200012), “IMI workshop II: Geometry and Algebra in Material Science II”, August 30-31, 2021”, (20210001), and “IMI workshop I: Geometry and Algebra in Material Science III”, September 8–10, 2022” (2022a003)). Y. K. has been supported by Grants: Young Scientist of Japan Society for the Promotion of Science Grant, no. JP 20K14312. S. M. has been supported by the Grant-in-Aid for Scientific Research (C) of Japan Society for the Promotion of Science Grant, No.21K03289. Y. O. has been supported by Grants: Young Scientist of Japan Society for the Promotion of Science Grant, no. 21K13799.

In the display of the atomic configurations, we used the visualization software, VESTA [30].

REFERENCES

- [1] H. Shima and S. Onoe. *Topology-Induced Geometry and Properties of Carbon Nanomaterials*, pages 53–84. Springer-Verlag, New York, the role of topology in materials edition, 2018.
- [2] H. Terrones and A. L. Mackay. Negatively curved graphite and triply periodic minimal surfaces. *J. Math. Chem.*, 15:183–195, 1994.
- [3] H. Terrones. Curved graphite and its mathematical transformations. *J. Math. Chem.*, 15:143–156, 1994.
- [4] M. Itoh, M. Kotani, H. Naito, T. Sunada, Y. Kawazoe, and T. Adschiri. New metallic carbon crystal. *Phys. Rev. Lett.*, 102:055703, 2009.
- [5] Y. Yao, J. S. Tse, J. Sun, D. D. Klug, R. Martoňák, and T. Iitaka. Comment on “new metallic carbon crystal”. *Phys. Rev. Lett.*, 102:229601, Jun 2009.
- [6] M Kotani, H. Naito, and T. Omori. A discrete surface theory. *Comput. Aided Geom. Design*, 58:24–54, 2017.
- [7] M Kotani, H. Naito, and C. Tao. Construction of continuum from a discrete surface by its iterated subdivisions. *Tohoku Math. J.*, 74:215–227, 2022.
- [8] T. Sunada. Lecture on topological crystallography. *Japan. J. Math.*, 7:1–39, 2012.
- [9] J. Onoe, T. Nakayama, M. Aono, and T. Hara. Structural and electronic properties of an electron-beam irradiated C₆₀ film. *Appl. Phys. Lett.*, 82:595–59, 2003.
- [10] S. Ueda, K. Ohno, Y. Noguchi, S. Ishii, and J. Onoe. Dimension dependence of the electronic structure of fullerene polymers. *J. Phys. Chem. B*, 110:22374–22381, 2006.
- [11] J. Onoe, T. Ito, H. Shima, H Yoshioka, and S. Kimura. Observation of riemannian geometric effects on electronic states. *Eur. Phys. Lett.*, 98:27001 (5pages), 2012.
- [12] T. A. Beu and J. Onoe. First-principles calculations of the vibrational spectra of one dimensional C₆₀ polymers. *Phys. Rev. B*, 74:195426, 2006.
- [13] Y. Noda, S. Ono, and K. Ohno. Geometry dependence of electronic and energetic properties of one-dimensional peanut-shaped fullerene polymers. *J. Phys. Chem. A*, 119:3048–30556, 2015.
- [14] V. M. Vassilev. Unduloid-like equilibrium shapes of single-wall carbon nanotubes under pressure. In *Fourteenth International Conference on Geometry, Integrability and Quantization June 8-13, 2012, Varna, Bulgaria*, pages 244–252, 2013.
- [15] S. S. Xie, W. Z. Li, L. X. Qian, B. H. Chang, C. S. Fu, R. A. Zhao, W. Y. Zhou, and G. Wang. Equilibrium shape equation and possible shapes of carbon nanotubes. *Phys. Rev. B*, 54:16436–16439, 1996.
- [16] Y. Kabata, S. Matsutani, and Y. Ogata. On discrete constant principal curvature surfaces. *arXiv:2306.15846*, 2023.
- [17] A. Takashima, J. Onoe, and T. Nishii. In situ infrared spectroscopic and density-functional studies of the cross-linked structure of one-dimensional C₆₀ polymer. *J. Appl. Phys.*, 108:033514 (5pages), 2010.
- [18] H. Masuda, J. Onoe, and H. Yasuda. High-resolution transmission electron microscopic and electron diffraction studies of C₆₀ single crystal films before and after electron-beam irradiation. *Carbon*, 81:842, 2015.
- [19] H. Masuda, H. Yasuda, and J. Onoe. Two-dimensional periodic arrangement of one-dimensional polymerized C₆₀ evidenced by high-resolution cryo-transmission electron microscopy. *Carbon*, 96:316–19, 2016.
- [20] G. Wang, Y. Li, and Y. Huang. Structures and electronic properties of peanut-shaped dimers and carbon nanotubes. *J. Phys. Chem. B*, 109:10957–10961, 2005.
- [21] Y. Noda and K. Ohno. Metallic and non-metallic properties of one-dimensional peanut-shaped fullerene polymers. *Synth. Met.*, 161:1546–1551, 2011.
- [22] G. Kresse and J. Furthmüller. Efficient iterative schemes for ab initio total-energy calculations using a plane-wave basis set. *Phys. Rev. B*, 54:11169–11186, 1996.
- [23] P. Hohenberg and W. Kohn. Inhomogeneous electron gas. *Phys. Rev.*, 136:B864–B871, 1964.

- [24] J. P. Perdew, K. Burke, and M. Ernzerhof. Generalized gradient approximation made simple. *Phys. Rev. Lett.*, 77:3865–3868, 1986.
- [25] G. Kresse and D. Joubert. From ultrasoft pseudopotentials to the projector augmented-wave method. *Phys. Rev. B*, 59:1758–1775, 1999.
- [26] H. Jensen and H. Koppe. Quantum mechanics with constraints. *Ann. Phys.*, 63:586–591, 1971.
- [27] R. C. T. da Costa. Quantum mechanics of a constrained particle. *Phys. Rev. A*, 23:1982–7, 1981.
- [28] S. Matsutani. Path integral formulation of curved low dimensional space. *J. Phys.Soc.Jpn.*, 61:53–63, 1992.
- [29] S. Matsutani. Quantum field theory on curved low dimensional space embedded in three dimensional space. *Phys. Rev. A*, 47:686–689, 1993.
- [30] K. Momma and F. Izumi. Vesta 3 for three-dimensional visualization of crystal, volumetric and morphology data. *J. Appl. Crystallogr.*, 44:1272–1276, 2011.

Yutaro Kabata
School of Information and Data Sciences,
Nagasaki University,
1-14 Bunkyo-machi, Nagasaki City 852-8131, Japan

Shigeki Matsutani
Electrical Engineering and Computer Science,
Graduate School of Natural Science & Technology,
Kanazawa University,
Kakuma Kanazawa, 920-1192, Japan
s-matsutani@se.kanazawa-u.ac.jp

Yusuke Noda
Department of Information and Communication Engineering,
Okayama Prefectural University,
111 Kuboki, Soja, Okayama 719-1197, Japan

Yuta Ogata
Department of Mathematics, Faculty of Science,
Kyoto Sangyo University,
Motoyama, Kamigamo, Kita-ku, Kyoto 603-8555, Japan

Jun Onoe
Department of Energy Science and Engineering
Nagoya University,
Furo-cho, Chikusa-ku, Nagoya, Aichi 464-8603, Japan